Available online at www.CivileJournal.org

Civil Engineering Journal

(E-ISSN: 2476-3055; ISSN: 2676-6957)

Vol. 11, No. 11, November, 2025

Behavior of Deep Beams with Different Proportions of Recycled Plastic Type HDPE Instead of Coarse Aggregate

Ahmed M. Abawi [1], Oday Asal Salih [1*]

[1] *Civil Engineering Department, College of Engineering, University of Mosul, Mosul, 41001, Iraq.*

Received 27 June 2025; Revised 18 September 2025; Accepted 04 October 2025; Published 01 November 2025

Abstract

One of the most appealing strategies in the ongoing effort to lessen humans' impact on the environment is using waste plastic as coarse particles in concrete. This innovative approach addresses the pressing issue of mounting plastic waste and aims to diminish the adverse effects of traditional building materials, such as natural aggregates, on the environment. Plastic waste as coarse aggregates exemplifies a professional dedication to creating a resilient infrastructure that mitigates environmental harm and contributes to a greener future for future generations. Eight deep beams were cast with sustainable concrete that was made from two mixtures: one in normal strength (C30) and the other in high-strength concrete (HSC) (1% Hyperplast PC200 of cement) that included HDPE plastic, which was taken from fruit boxes that had been crushed and used in 10, 20, and 30 percentage volumetric proportions as a substitute for coarse aggregate. The two still intact have no HDPE replacement and serve as each deep beam's reference deep beam. Shear failure and ductility in the second group were slightly lower than 2% compared to the reference beam for B30. It can be argued that while the replacement has positive environmental impacts, the 23.5% loss in strength is unwanted, while the 2% decline in ductility is acceptable. While maintaining a competent structural flexural behavior, the first group demonstrated an increase in shear failure by the replacement rate (20%, 30%), and the 10% replacement rate dropped by a tiny percentage (1.25%) in comparison to the reference specimen.

Keywords: Reinforced Concrete; Deep Beams; Sustainable Concrete; Recycled HDPE Plastic.

1. Introduction

The rapid development of the global economy has led to a significant increase in the demand for various industrial materials essential for daily demands. This rise of the industrial sector has two adverse consequences on the environment. Initially, as the industrial industry expands, the need for energy increases, resulting in elevated carbon dioxide emissions. Manufacturing and transporting one ton of plastic resin emits about 2.5 tons of CO_2 into the atmosphere [1]. Secondly, the materials that are produced are frequently thrown away, used only partially, or used for a brief time. Consequently, the waste generated from these materials necessitates processing and disposal, thus impacting the environmental conditions of the treatment zone (water, air, and soil). Sustainable practices have emerged as the most effective technique for reducing the impact of these two primary adverse consequences. These practices involve the utilization of wastes from industrial production as replacements for resources utilized in other industries. The preservation of the environment and the prevention of the exhaustion of natural resources for use by other companies are both facilitated by this. Plastic is one of the materials created most frequently and is consequently employed in everyday life. Plastic is utilized in the production of disposable objects for a wide range of applications [2, 3].

* Corresponding author: odaycivileng@uomosul.edu.iq

http://dx.doi.org/10.28991/CEJ-2025-011-11-03

Investing in a circular system to control plastic pollution presents viable remedies that positively affect the environment and society. Reintroducing wasted plastics back into the supply chain will preserve their value and cut down on the amount of plastic waste that ends up in the environment. As a result, it's essential to identify a pertinent local trash strategy that addresses plastics and to customize partnerships to meet the needs of different stakeholders, including companies, industries, and civil society [4]. Establishing a connection between the waste and construction sectors seems to be one approach to improving the circularity of plastics, especially the widely used macro-plastics [5]. Their usage as an additive in concrete mixes might yield additional value and open up new commercial prospects [6]. The study's results indicate that parking lots, walkways, and wall panels are among the non-structural projects where plastic additives in concrete will be mainly used [7]. In an experimental investigation, Al-Darzi et al. tested eight reinforced concrete slabs, divided into four groups of two slabs each, exposed to impact stress with aggregate replaced by 0%, 4%, 8%, and 16% polyethylene terephthalate.

PET polymers increased fresh concrete workability by 16% and lowered density by 9% during preparation. The compressive strength fell 11.7%, 15.7%, and 19.9% with 4%, 8%, and 16% PET. The splitting strength was reduced by 7.2%, 17.4%, and 20.3% with 4%, 8%, and 16% PET. The failure mechanism and deflection amplitude showed that PET delayed the beginning of the first fractures and reduced crack length, width, and propagation at failure. PET enhanced impact resistance during the first fracture and ultimate load phases compared to standard concrete.

The highest and lowest displacements were reduced when PET reached 8% and 16%. With four-node shell components, SAP2000 mimicked the slabs. The FE analysis showed a similar deflection reaction to the experiment for all slabs. FE showed lesser deflections of 15.5% and 19% than other experimentally tested slabs, except for slab G2-2, which showed 16.3% [8]. Research by Hassan et al. examines the shear behavior and strength of concrete beams reinforced with BFRP bars using experimental and computational methods. The effects of straps, water bottles, and ropes on beam performance were examined. The study focuses on fiber aspect ratio and material composition. These impacts were tested on seven concrete beams and confirmed by ABAQUS finite element analysis (FEM). Recycled plastic fibers did not significantly increase the shear strength of fiber-reinforced concrete (FRC) beams, except for the BFRP beam with 20 mm short water bottle fibers, which increased shear strength by 13.97%. Analytical findings matched experimental data on failure load, cracking behavior, and deformation behavior, suggesting strong agreement between the two methods [9]. One of the solutions is reinforced concrete deep beams, which have many beneficial uses in buildings and bridge structures like transfer girders, wall footings, foundations, floor diaphragms, bunkers, and tanks because of their large concrete size and capacity to hold a large amount of plastic. Deep beams are often used in the lowest floors of tall constructions for residential and commercial applications [10-13]. If a beam's depth is greater than its span, it is referred to as a deep beam. As stated in ECP 203-2018 [14]. The optimal span-to-depth ratios for deep beams are below 1.25 for simple beams and 2.50 for continuous beams. According to ACI 318-19, the definition of a deep beam differs [15]. Deep Beam: A structural component subjected to concentrated stresses positioned at a distance equal to or less than twice its depth from the support face, or with a clear span equal to or less than four times its total depth. The strength characteristics and material properties of a deep beam dictate its performance.

Rahim et al. found that concrete incorporates high-density polyethylene (HDPE) plastic trash as coarse aggregates at replacement rates of 10%, 20%, and 30%. Conducted compressive strength, water absorption, and slump tests in the laboratory for this inquiry. Samples with 10% HDPE demonstrate enhanced strength performance [16]. Shanmugapriya & Santhi's study looks at concrete's mechanical and chloride permeability properties that incorporate a significant amount of high-density polyethylene (HDPE) waste instead of fine and coarse particles. Using HDPE trash in place of part of the sand (5, 10, 15 percent) and gravel (10%, 15%, 20%), six different M25 grade mixes of concrete were produced. Regarding split tensile and compressive strength, the behavior of the concrete mixes, using differing quantities of HDPE waste as a substitute for natural aggregates, is like that of the conventional cement concrete mix. Conversely, mixes containing waste HDPE have superior flexural strength characteristics compared to ordinary cement and mixes of concrete. The incorporation of HDPE trash reduces the concentration of chloride ions that infiltrate, as indicated by the quick findings for chloride permeability. As a result, the mixtures were classified as having moderate permeability compared to cement concrete, exhibiting significant permeability. The research indicates that waste plastic may be reclaimed and used as a replacement for aggregates in concrete, which would significantly lessen disposal issues [17]. Punitha et al. [18] did the research. The high-density polyethylene (HDPE) plastic powder is combined with the fine aggregate and cement in six different proportions: 5%, 10%, 15%, 20%, 25%, and 30%. Additionally, 10% metakaolin is also included in the mixture. The use of 10% metakaolin and 15% HDPE plastic powder in the concrete yielded superior compressive strength compared to conventional concrete. Experimental data indicate that the use of 10% metakaolin and 5% HDPE plastic powder in concrete may substitute up to 80% of flexural strength and 90% of split tensile strength [18].

Tamrin & Nurdiana conducted a study where they incorporated high-density polyethylene (HDPE) plastic trash into concrete mixtures. The plastic waste was added at different percentages: 2.5%, 5%, 10%, and 20% based on the weight of the cement. The HDPE lamellar particles had dimensions of 10 by 10 mm, five by 20 mm, and 2.5 by 40 mm, with a thickness of 0.5 mm. The research indicated that the medium concrete class, with a compressive strength of 10 MPa,

had the most advantageous reaction to the inclusion of HDPE. Ideal dimensions for all varieties of concrete were 5 × 20 mm, and the optimal composition included (5%) HDPE [19]. Radhi et al. study test beams, with dimensions of (2000 mm) in length and (180 × 280 mm) in cross-section, underwent bending loads applied at four points. A mixture of high-strength concrete (HSC) and vegetable carton shreds of high-density polyethylene (HDPE) plastic was used to make sustainable concrete in place of three beams. The proportion of HDPE utilized in the concrete was ten, twenty, and thirty percent. The fourth beam, devoid of any HDPE replacement, is the reference beam. The test findings revealed that despite the toughness of the (30%) replacement beam increased by (24%, its capacity to support weight decreased by 7%. The failure time and cracking mechanism were comparable to the reference beams. These findings hold great promise for understanding a (30%) partial substitution of natural coarse aggregate with HDPE plastic while preserving structurally sound flexural performance [20].

Following the enumeration of prior investigations, each researcher conducted their investigation, focusing on aspects such as beam type, behavior, or the quality of recovered plastic. Most researchers typically understood the behavior of deep beams in isolation from recycled plastic (without plastic) or in relation to the behavior of concrete or conventional beams using recycled plastic and various kinds of plastic, and they did not analyze the performance of the deep beam using recycled HDPE plastic. This research seeks to assess the efficacy of plastic waste as a partial substitute for coarse aggregate in structural concrete. The evaluation was conducted on a structural scale using reinforced concrete deep beams, measuring 1500 mm in length. The beams featured a cross-section of 150 mm by 500 mm and incorporated plastic waste aggregate. Consequently, an examination of the influence of microplastic debris on the structural performance of reinforced concrete deep beams was performed.

2. The Experimental Work

2.1. Prepare Materials and Mixtures

Ordinary Portland cement from nearby manufacturers was utilized for all of the mixtures in this experiment. The cement's physical characteristics and chemical makeup, meeting the requirements of IQS:5/2019 [21], are shown in Tables 1 and 2, which were prepared per Iraqi Standard No. 5/2019. Hyperplast (PC200), an additional binder, was also added in the combinations used in this investigation. This experiment used 1.0 liter of cementation material per 100 kg. Hyperplast (PC200) is a high-performance superplasticizer composed of long-chain polycarboxylic polymers, designed to enhance the water content efficiency of concrete. This effect can achieve the best durability and performance with flowable, high-strength concrete mixes with the technical attributes indicated in Table 3. Local natural gravel from the area served as the coarse aggregate in the mixture, and regional natural sand from Mosul City served as the fine aggregate. Fine aggregates had maximum particle sizes of 4.75 mm, whereas coarse aggregates had maximum particle sizes of 12.5 mm.

In order to examine the attributes of the sand and gravel, the sieve analysis in Figure 1 and Iraqi Standard No. 45/1984 were utilized. Table 4 presents a catalog of the physical properties of the sand and gravel used. Before they applied for the removal of dust and other pollutants from the particle surfaces, both aggregates were meticulously cleaned and allowed sufficient time to dry on the surface. The veggie plastic boxes in Figure 2-a were used to produce the recycled plastic coarse aggregate employed in this experiment. The boxes were first gathered and rudimentarily fragmented into bits resembling the coarse aggregate used in the building sector. The plastic boxes were cut into small pieces with the shredding device shown in Figure 2-b, as shown in Figure 2-d; the necessary quantity of recycled plastic pieces was collected (Figure 2-c), cleaned, and let air dry before being sieved via typical coarse aggregate sieves. The plastic pieces were mostly flat in shape, though their color and shapes varied according to the color of the source box and its parts. The physical characteristics of the regenerated plastic waste aggregate are enumerated in Table 5, as per Exhibit Iraqi Standards No. 45/1984 pertaining to the grading of fine aggregate, coarse aggregate, & coarse recycled plastic aggregate, respectively, in Figure 1.

Table 1. Physical Properties of Cement

Physical Properties	Results	Specifications (IQS:5/2019) [21]
Initial Setting Time (minutes)	120	≥ 60
Compressive Strength 2 days (MPa)	22.8	≥10
Compressive Strength 28 days (MPa)	43.0	≥42.5
Standard ductility	0.28	-
Final Setting Time (hrs.)	4:15	≤10
Fineness Sieve no. 170 (%)	2.5	≤10
Le Châtelet method expansion (mm)	2.0	≤10

Table 2. Chemical Properties of Cement

Properties of Chemical	Results	Specifications (IQS:5/2019) [21]	Properties of Chemical	Results
MgO	2.49	≤ 5%	SiO_2	21.30
SO_3	1.91	≤ 2.5% if C3A≤ 5%	Al_2O_3	5.16
Free lime	1.46	≤2.8% if C3A≤ 5%	Fe_2O_3	4.52
Loss on ignition	1.29	0.66-1.02	Cao	63.87
Insoluble residue	1.17	≤ 4%	C_2S	26.68
C_3A	6.03	≤ 3.5	C_3S	45.59
L.S.F	90.93	-	C_4AF	13.75

Table 3. Technical Characteristics of Hyperplast (PC200) at 25 ºC

Properties	Results
Freezing Point (ºC)	-3ºC
Color	Liquid with a light-yellow color
Air Entrainment	At regular doses, less than 2% air is entrained above the control mix.
Specific Gravity	1.05+0.02

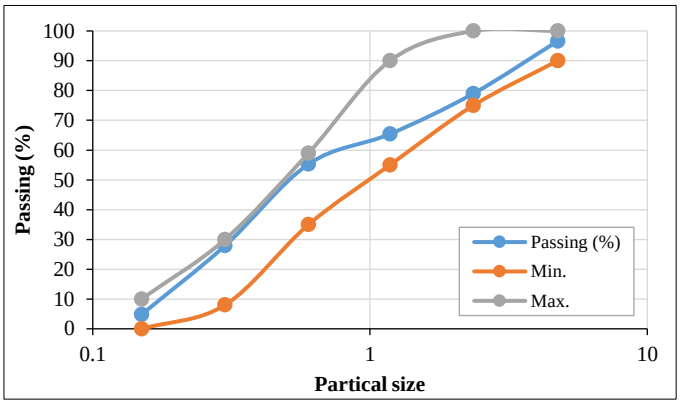

(a) Sieve analysis of fine aggregates

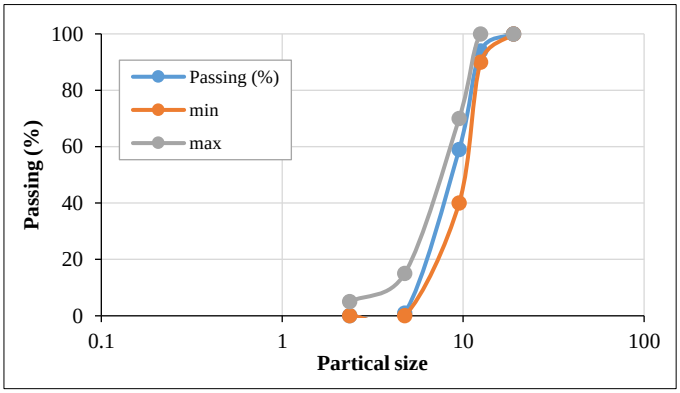

(b) Sieve analysis of coarse aggregates

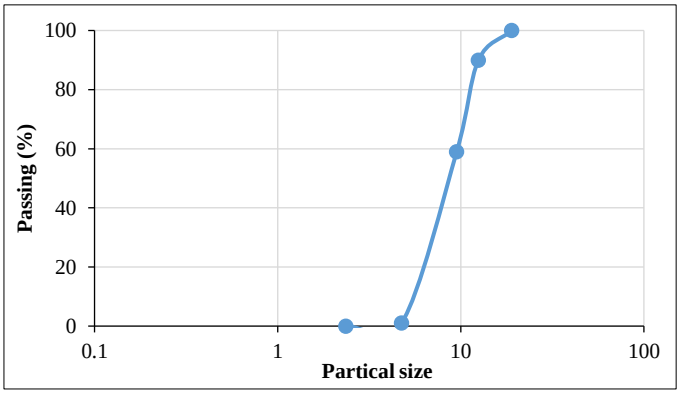

(c) Sieve analysis of recycled plastic coarse aggregates

Figure 1. Diagram of Sieve analysis for the used materials

Table 4. Fine/Coarse Aggregate Physical Properties

Physical Properties of Fine Aggregate	Results	Iraqi Standard No. 5 /1984	Physical Properties of Coarse Aggregate	Results	Iraqi Standard No. 5 /1984
Density (kg/m^3)	2.68	-	Density (kg/m^3)	2.623	-
Sulfate Content (%)	0.15	≤0.5	Sulfate Content (%)	0.030	≤ 0.1
Porosity (%)	2.64	-	Porosity (%)	2.05	-
Specific Gravity	2.60	-	Specific Gravity	2.60	-

(a) Unprocessed plastic container

(b) Fragmentation

(c) Gathering fragmented sections

(d) Sieve analysis

Figure 2. Procedure for making coarse aggregate from plastic waste

Table 5. Physical Characteristics of the Coarse Recycled Plastic Aggregate

Property	Value	ASTM Standard
Density (in kg/m^3)	0.95	ASTM D792-20
Compressive Strength (in MPa)	26.4	ASTM D695-15
Water Absorption	0	ASTM D570-98R18
Modulus of Elasticity (in MPa)	358.7	ASTM D638-14
Tensile Strength (in MPa)	7.7	ASTM D638-14
Flexural Strength (in MPa)	878.3	ASTM D790-17

Grade 60 deformed reinforcing steel bars in a range of diameters were used in the studs' reinforced concrete beams. The tensile bars were 12 mm in diameter (Grade 60), while the upper holding bars of the beams were 8 mm (Grade 60) bars. On the other hand, in order to maintain diagonal tension and meet shear requirements, 8 mm diameter bars were also employed as webs and stirrups. In compliance with ASTM A615-16, samples from the three bars were analyzed in the laboratory. The outcomes of the physical property tests for bars are summarized in Table 6. In an attempt to create a concrete combination that would be exceptionally workable and strong enough to be used in structural applications, many trial mixtures were cast and evaluated. Following the selection of the optimal mixture, two additional trial mixes (30 and 45 MPa) were cast and tested to determine the impact of the recovered plastic waste on the workability and strength of the mixture. In addition to the reference mixture containing no plastic waste, three combinations were assessed for each mixture (30 and 45 MPa), with three percentage substitutions of 10, 20, and 30% of plastic waste recovered by natural gravel. The details of the eight blends are listed in Table 7. Note that B0 represents the reference combination with no recycled plastic waste, and B10, B20, and B30 represent blends with 10%, 20%, and 30% substitution of the recycled plastic waste, respectively.

Table 6. Characteristics of Steel Bars Reinforcement

Nominal Diameter (mm)	Dia. 8 mm	Dia. 12 mm
Actual Diameter (mm)	8.08	11.67
Yield Stress (MPa)	420	496
Ultimate Strength (MPa)	564	577
Total Elongation (%)	26	16

Table 7. Proportions of Mix

Mixture	Cement (kg/m^3)	Sand (kg/m^3)	Gravel (kg/m^3)	Water (kg/m^3)	Hyperplast PC200 (kg/m^3)
C30	350	850	950	165	0
C45	450	800	900	150	4.5

2.2. The Instruments and Equipment

The following sections will provide a detailed illustration of the instruments and equipment utilized to evaluate the beam specimens.

2.2.1. Linear Variable Differential Transformer LVDT

The Linear Variable Differential Transformer determines the displacement for the structural member by converting the movement into an electrical signal that the data logger attached to it can read. As seen in Figure 3-a, it is positioned below the beam in the center span to determine the beam's most excellent deflection at this location.

2.2.2. Load Measurement Device

The test-applied load values were computed using an electrical load cell with a 1000 kN capacity. The load cell utilized in the experimental test is shown in Figure 3-b. The load was measured from the commencement of the test to the failure load using a data logger device.

2.2.3. Data Logger

It (Figure 3-c), an electrical device with a specific computer application installed, analyzes the data from the devices linked to it and extracts it as an Excel sheet file. The load cell and LVDT were all connected to 16 channels of the data logger employed in this investigation.

2.2.4. Test Frame

In Figure 3-d, the beams are tested using a large steel frame, which was intended to test supported beams.

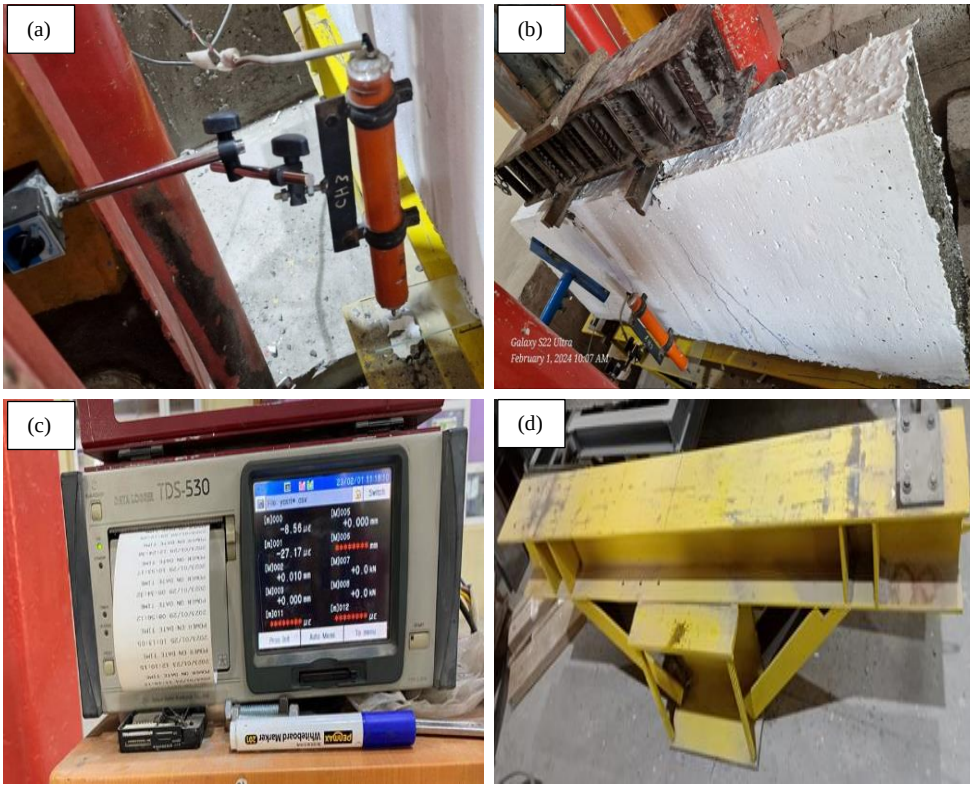

Figure 3. (a) LVDT, (b) Load Measurement Device, (c) Data logger, (d) Frame supported

2.2.5. Test System

In the structural lab, all specimens are methodically sorted following their groupings. After being transferred and raised to the machine, the beams are subjected to a 4-point force delivered in increments of 5 kN. A load cell attached to a computerized data recorder measures monotone point loads applied to the beam. Concrete strain gauges are connected to the same electronic data recorder, which measures deflection, tension, compression, and steel reinforcing stresses. Data logger device results for load and deflection at the crack, ultimate, and fail phases.

2.3. Setup Reinforced Concrete Deep Beams

Under investigation in this study are reinforced concrete deep beams that were constructed in accordance with ACI 318-19 specifications for failure in flexure. The beam's cross-section measured (500 mm) in depth and (150 mm) in width. Its entire length measured 1500 mm. Consequently, the steel ratio was around 0.33% for compression and 0.14% for tension. 2Ø8 mm top bars and 2Ø12 mm bottom tension were employed to reinforce each beam. In contrast, (Ø8 mm) closed stirrups and webs were positioned along the spans at a distance spacing of (225 mm) to avoid shear failure. There was an adequate depth of 450 mm with a concrete bottom cover measuring 25 mm. Eight similar deep beams were produced using the two mixtures of concrete in Table 7. The specimens and the mixes have the same identifying number since the primary goal of the testing is to determine how using recycled plastic waste affects the flexural performance of deep beams. The geometric characteristics and steel of reinforcing concrete deep beams are shown in Figure 4. Using plywood forms held up by plates, the concrete deep beams were cast and then covered in water for twenty-eight days at a roughly twenty-five °C temperature. Figure 5 depicts the arrangement of the deep beam forms as well as the common concrete test molds that were created, inspected, and used in connection with each deep beam and the components that it needed.

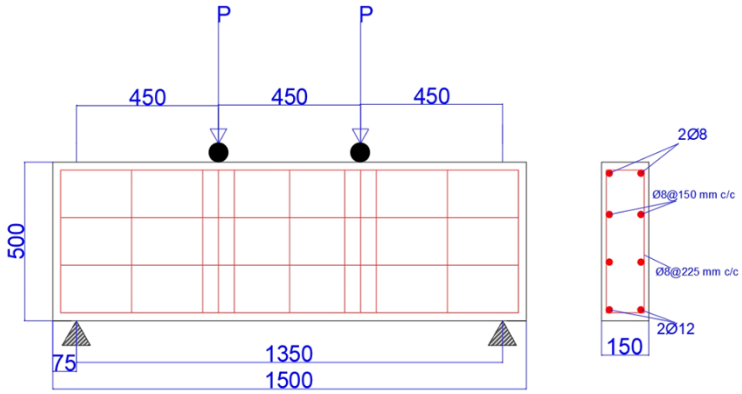

Figure 4. Concrete Beam Geometry and Reinforcement (all dimensions are mm)

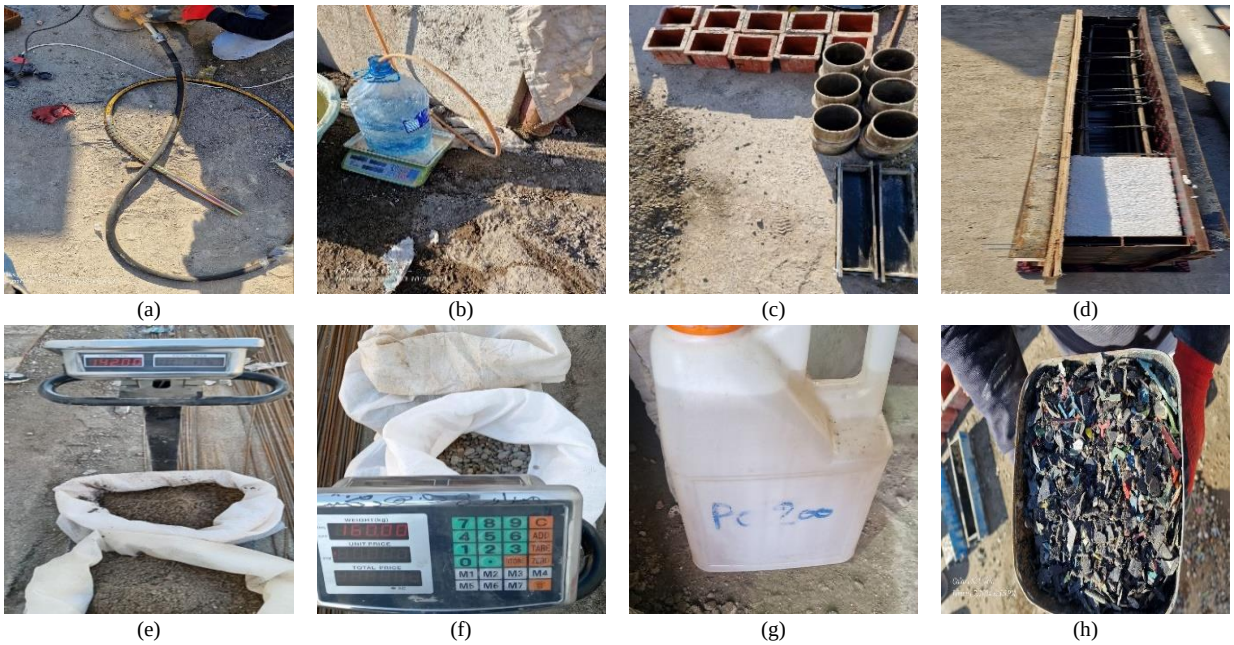

Figure 5. Formwork for reinforced concrete beams and test moulds, and whatever else is needed: (a) prepare vibrator before casting, (b) weighting the water, (c) prepare test moulds before test, (d) supply moulds of deep beam, (e) weighting sand, (f) weighting gravel, (g) supply superplasticizer, (h) supply recycled plastic.

2.4. The Configuration of the Test

As seen in Figure 6, the deep beams were subjected to the four-point bending test over a relatively straightforward span. When the length of the test span was 1350 mm and the distance between the 2-points of load was 450 mm, the length of each shear span was 450 mm. The force was supplied steadily and consistently using the hydraulic testing apparatus, and cracking was detected at every load level. According to the data presented in Figure 6, the load was quantified using a load cell with an output of one thousand kilonewtons, and the middle of span deflection was measured with a "linear variable differential transformer" (LVDT). A customized data logger was used to gather and log the data from the load cell simultaneously, as well as the lower voltage differential transformer (LVDT) and the strain gauges. Figure 6 shows that reinforced concrete deep beams designed for flexural testing are available.

Figure 6. Reinforced Concrete Deep Beam Test Setup

2.5. Research Methodology

Figure 7, shows the flowchart of the research methodology through which the objectives of this study were achieved:

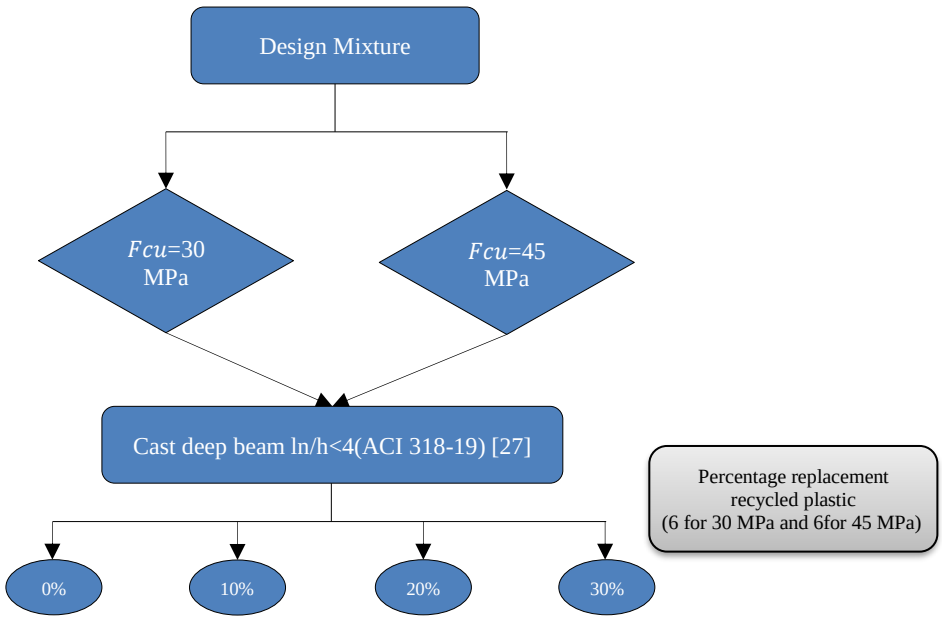

Figure 7. Flowchart of the methodology

3. Results and Discussion

Investigations were conducted into the ultimate load, cracking loads, deflection response, and other structural quality factors. The study factors, such as the amount of waste plastic in the two groups of compressive strength (30 and 45 MPa), were the basis for the results. Table 8 provides specifics about the test results.

Table 8. The Experimental Test Results

Specimens	Group	Deep beam symbol	Plastic waste	Failure Loads (kN)	First Crack load (kN) (1st stage)	Maximum Deflection (mm)	Ductility Index (DI)	Stiffness, K (kN/mm)	Failure Mode
B0	C30	B0	0%	320	250	2.86	1.66	103	Shear
B10		B10	10%	316	250	1.53	1.08	135	Shear
B20		B20	20%	344	239	2.59	2.84	212	Shear
B30		B30	30%	353	240	4.55	2.13	88	Shear
B0	C45	B0	0%	458	240	17.15	6.42	106	Shear
B10		B10	10%	391	250	6.91	2.82	116	Shear
B20		B20	20%	446	250	8.69	3.34	90	Flexural
B30		B30	30%	350	235	2.21	1.27	128	Shear

3.1. Patterns of Cracking and Failure

A significant crack between the support and bearing zones was the reason the specimens failed. In the majority of the samples, the first apparent break was a little bending crack that ran between the two stress zones in the center (Figure 8). Due to the plasticizer it contained, in group C45, specimen B30 was the sample with the lowest apparent because the plasticizer worked to lift most of the plastic strips (due to their light weight), and there was no alternative to the coarse aggregate in the lintel. Measuring around 235 kN from the center to the bottom. Because of its low weight, this plasticizer helped the waste plastic bits rise to the top. However, because there isn't enough plastic in the world, fissures don't form. With the exception of the group C45 specimen B20 specimen, which failed via flexure, oblique shear fractures started after the initial breaking and progressively spread from the supports toward the loading sites. The more force applied, the larger these fissures become. Following that, a failure occurred at 320 KN of load. The diagonal shear fracture in the group C30 specimen B0 model failed, causing the beam to split into two halves. Table 8 and Figure 8 (C30), respectively, demonstrate that in the first group's mix, as the percentage of plastic waste increased to 20% and 30%, the load failure decreased by 1.25% due to the non-uniformity of the plastic. It is sufficient with the concrete mix, while the load increased by 7.5% and 10.3% due to the plastic's resistance to cracks and its homogeneity with the concrete mix. This plasticizer worked to raise the plastic waste to the surface because it is light in weight, as shown in Figure 9. Within the two groups, the source failure was recorded at a magnitude of 458 kN; it decreased by 14.6% when the percentage of replacement of plastic waste rose to 10%; the load was observed to decrease by 2.6% and 23.5% when the rate of plastic waste increased to 20% and 30%, respectively. Notwithstanding the rise in plastic garbage, the load is diminishing. Unlike the first group, the load escalated with the rising quantity of plastic waste. The presence of the plasticizer, which enabled some plastic debris to ascend to the surface and led to inadequate integration of the plastic with the concrete mixture, caused the decline, as shown in Figure 9.

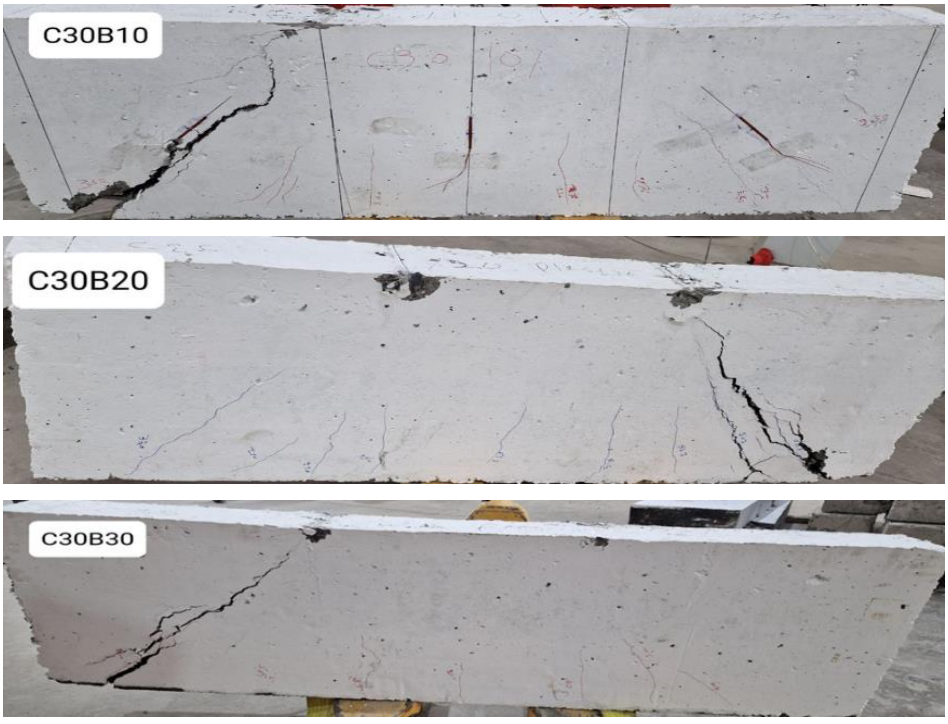

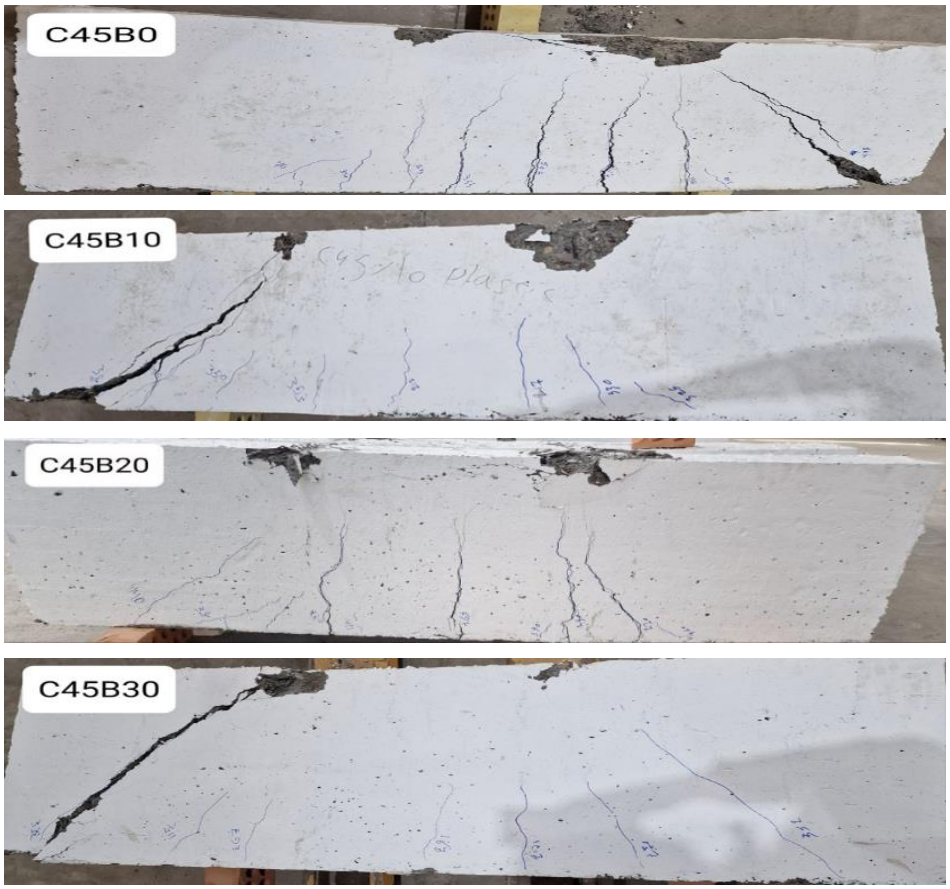

Figure 8. Deep beams of reinforced concrete display cracking patterns

Figure 9. During Casting, Plastic Trash Rises to the Surface

3.2. Behavior of load-deflection

A diagonal fracture between the loading and supporting sections failed the control specimen, Group C30 specimen B0. First, a short flexural fracture between the two loading zones in the mid-section at 250 kN bottom stress was noticed. After the 250 kN load, inclined shear fractures propagated from the supports to the loading direction. Higher loads cause bigger fractures. Figure 10-a shows that a diagonal shear fracture failure at 320 kN splits the beam into two. Figure 11 shows load-deflection curves for Group C30 specimen B0. The test examined how 10% recycled plastic by volume of coarse aggregate affected the specimen's shear characteristics, Group C30 specimen B10. A little flexural fracture and the first crack appeared between the two loading zones in the center of the span at 250 kN. Shear cracks grow with stress after 250 KN loading. Figure 10-a shows that the beam fractured at 316 kN of shear stress, causing diagonal shear fractures. The Group C30 specimen B10 beam's shear capability drops 1.25 percent when recycled plastic is used. The original crack's appearance stayed the same; however, the values relative to Group C30 specimen B0 rose by 10% as HDPE recycled plastic increased. Figure 11 shows load-deflection curves for 10% recycled plastic. Figure 11 shows load-deflection curves for specimen Group C30 and specimen B20. 20% recycled plastic was tested on deep beam structural capabilities. A little flexural fracture at 239 kN was the first visible crack between the two loading zones in the center of the span. When loaded to 239 kN, shear fractures propagate and widen. Figure 10-a shows diagonal shear fractures breaking the beam at 344 kN. The results show that 20% recycled plastic enhanced shear capacity by 7.5% over Group C30 specimen B0. For deep beams, a 20% increase in HDPE recycled plastic decreased the first fracture load by 4.4% compared to the Group C30 specimen B0. Using specimen Group C30 specimen B0, the research examined how 30% recycled plastic affected deep beam structural capabilities. First flexural fractures appeared at a load of 240 kN between the two -50 loading zones in the mid-span. Then, the shear fractures grew and progressed toward the loading and supporting points.

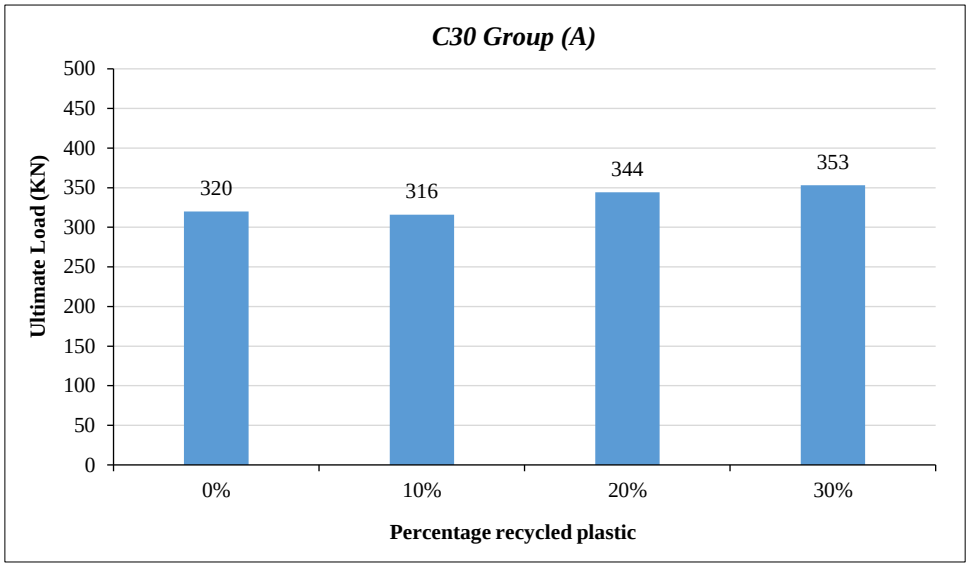

(a) The ultimate load of C30 Group(A)

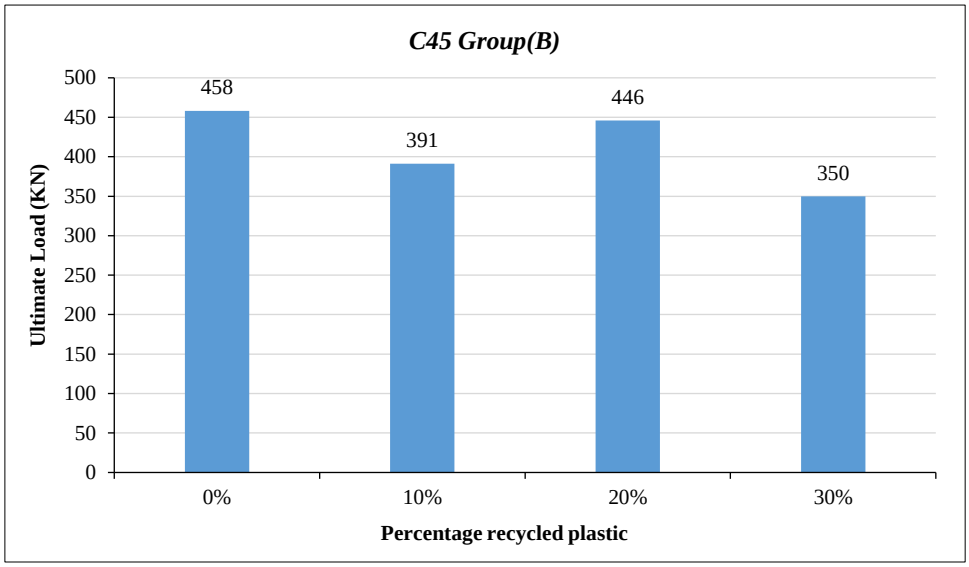

(b) The ultimate load of C45 Group(B)

Figure 10. The ultimate load of the beams

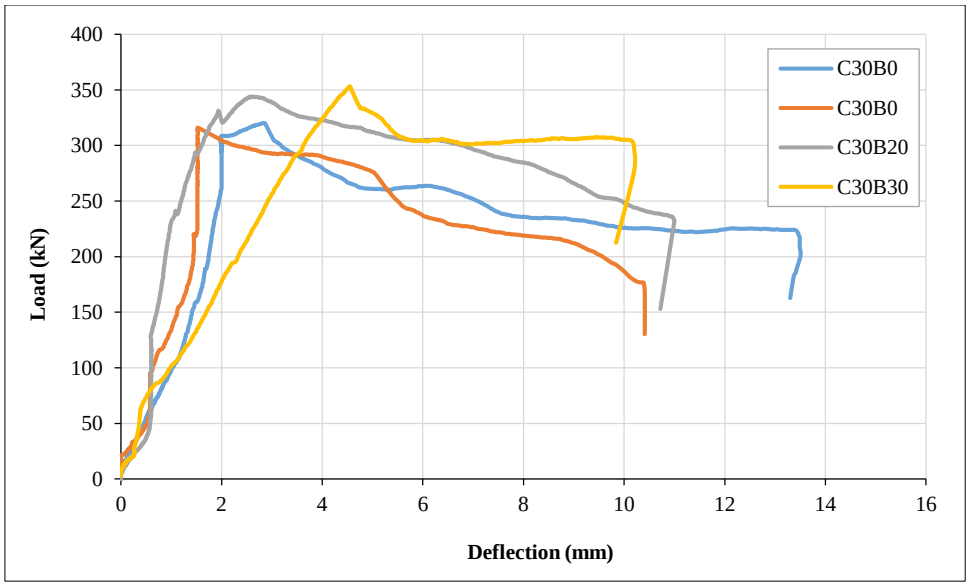

Figure 11. Load-Deflection Curves of the Reinforced Concrete Deep Beams, Group One C30

A few flexural fractures appeared at 250 kN. Figure 10-a shows that diagonal fissures in a top-separating concrete layer collapsed the specimen at 353 kN. When 30% recycled plastic was added, shear capacity increased by 10.3% compared to the Group C30 specimen B0. Deep beams made of 30% HDPE had a 4% lower first fracture load than Group C30 specimen B0. Figure 12 shows load-deflection curves. As stated in Table 8, Group B will explain the repaired beam specimen (C45) experimental results. Cracks between the loading and supporting sections caused the control specimen, Group C45 specimen B0, to fail. First, a short flexural fracture between the two loading zones in the center at 240 kN bottom stress was noticed. After the 240 kN load, inclined shear fractures developed and spread from the supports toward the loading area. Widening fissures increase stress. Figure 10-b shows the diagonal shear fracture failure that split the beam in two at 458 kN. Figure 12 shows load-deflection curves for it. Testing examined how 10% recycled plastic by volume of coarse aggregate affects Group C45 specimen B10 shear properties. In the middle of the span between the two loading zones, a 250 kN stress caused a fracture and a little flexural crack. After 250 KN, shear cracks develop with stress. Figure 10-b shows diagonal shear fractures from the beam breaking at 391 kN of bending stress. As shown, substituting recycled plastic reduces Group C45 specimen B0 beam shear capacity by 14.62%. When HDPE content rose by 10%, early crack load increased by 4.16% compared to the Group C45 specimen B0.

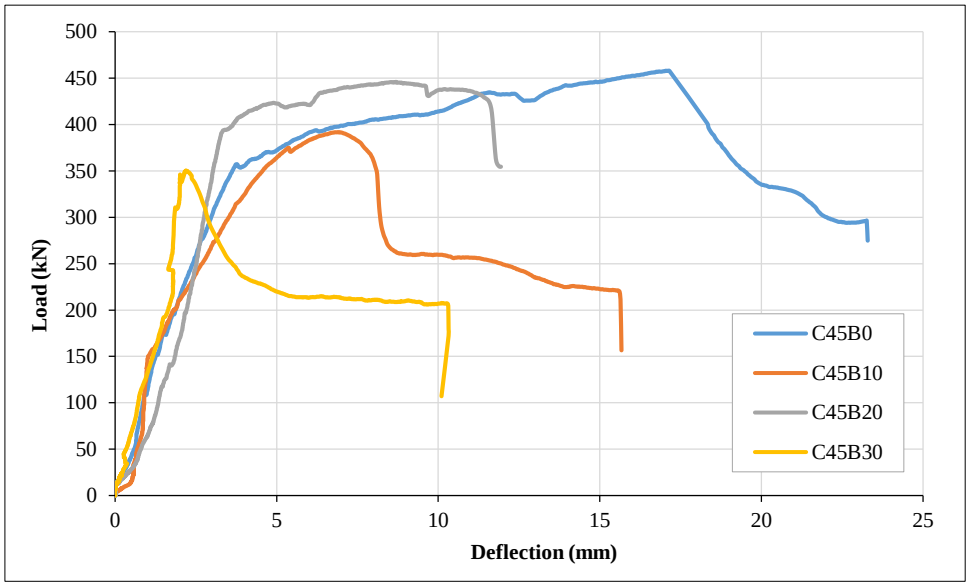

Figure 12. Load-Deflection Curves of the Reinforced Concrete Deep Beams, Group Two C45

Figure 12 illustrates load-deflection curves for using Group C45 specimen B0; 20% recycled plastic was tested on deep beam structural capabilities. The first visible flexural fracture between the two loading zones in the center of the span occurred at 250 kN. Once 250 kN is added, shear fractures spread and widen. The beam failed due to flexural failure fractures at 446 kN, as shown in Figure 10-b. Replacement of coarse aggregate with recycled plastic (20% by volume) reduced failure capacity by 2.62% compared to Group C45 specimen B0. Furthermore, compared to Group C45 specimen B0, a 20% increase in deep beam (HDPE) recycled plastic percentage increased the first crack load by 4.16%. Figure 12 illustrates load-deflection curves for Group C45 specimen B20. Using Group C45 specimen B30, the deep beam's structural strength was examined after substituting 30% recycled plastic with recycled plastic concrete. First flexural fractures appeared between the two loading zones in the mid-span at 235 kN. Then the shear fractures expanded and progressed quickly toward loading and supporting locations. Flexural fissures appeared at 235 kN. As illustrated in Figure 10-b, diagonal fissures pierced a layer of concrete that separated at the top, causing the specimen to collapse at (350) kN. Compared to Group C45 specimen B0, 30% recycled plastic coarse aggregate lowers shear capacity by 23.58%. Deep beams made of 30% HDPE had a 2.08% lower first fracture load than Group C45 specimen B0. Figure 12 illustrates load-deflection curves for Group C45 specimen B30. Final failure values varied. As illustrated in Figure 9, the plasticizer increased failure resistance and plastic percentage distribution by making certain plastic pieces light and ascend to the top. As the plastic percentage rises, compressive strength decreases, which affects shear failure.

3.3. Impact of Recycled Plastic on the Shear Strength Characteristics of Deep Beams

The primary objective of this experiment is to assess the impact of recycled plastic (HDPE) on the shear strength of reinforced concrete deep beams. The results shown in Figure 10 and Figures 11 and 12 indicate that including recycled plastic into concrete enhanced the shear strength of the beams and made the brittle shear failure more ductile at all percentages of recycled plastic. The ultimate load is recorded, and now the first fracture load manifests during the test. It further records the deflection value for each 10 kN increment in applied stress until the beam succumbs to failure. Figure 10 illustrates the first fracture load and ultimate load of the beams in detail. The results confirm that, despite a

slight increase in recycled plastic proportions, the first fracture load for beams in Group B has risen. This elucidates how the recycled plastic enhanced the interconnectivity of the concrete matrix and imparted significant tensile strength prior to the initiation of the first fracture. This elucidates how the recycled plastic enhanced the interconnectivity of the concrete matrix and imparted significant resistance to tensile loads prior to the formation of the first fracture. Likewise, several fractures are present instead of one, which is seen even inside the bending zone (between two significant loads). The use of recycled plastic likely contributed to the early fracture load increases in beams from Groups A and B by inhibiting crack propagation and controlling their expansion inside the beam. Furthermore, they may resist force and delay the emergence of fractures, enabling specimens to sustain substantial loads and deform before collapse. Figures 11 and 12. The use of recycled plastic, which is homogenous with the concrete mix and crack-resistant, resulted in an increase in load by 7.5% and 10.3% for the deep beams of Group A (B10, B20, and B30) and their ultimate loads, as seen in Figure 12. The load failure was reduced by 1.25% due to the heterogeneity of the recycled plastic, including a 10% inclusion of recycled plastic in the concrete mix, which is sufficient. When the proportion of recycled plastic replacement is elevated to 10%, as indicated by the findings of Group B's deep beams (B10, B20, and B30), the load diminishes by 14.6%; with increases to 20% and 30%, the load subsequently decreases by 2.6% and 23.5%, respectively, in comparison to Group C45 specimen B0. In Groups (A) and (B), the optimal load was seen at a recycled plastic percentage of 30%, with the ultimate load for the beam in Group (A) increasing by 10.3%. Recycled plastic may augment the tensile properties of concrete and inhibit fracture propagation inside the structure, hence boosting the ultimate load capacity of beams. Nonetheless, the reduction in the ultimate load at a recycled plastic percentage of 10% in group A may have resulted from the concrete's diminished workability, increased porosity, and reduced density, or the mixture's homogeneity, causing the recycled plastic to clump together [22].

3.4. Index of Ductility

In structural engineering, ductility is broadly defined as a member's capacity to undergo deformation when a load is applied continuously after reaching its maximum stage [23, 24]. Figure 13 displays the study's ductility index. According to the findings in Figure 10, at 20, 30% plastic waste as opposed to 0%, group C30's deep beams' ductility improved. At 10%, it's the least because, as we previously demonstrated, the plastic trash was not well combined with the mixture. The reinforced concrete member's increased ductility, which can withstand significant deflections before failing [25], indicates that the issue of rapid shear failure is lessened by waste plastic (HDPE). Because the second group (C45) is a combination with high resistance, the rise in plastic waste resulted in a loss in ductility because most of the plastic pieces floated to the top due to the plasticizer that makes light elements float. As shown in Figure 9, the percentage of plastic in these models became very small, so the ductility decreased. This mixture's primary purpose is resistance rather than ductility; the plastic component disrupts ductility.

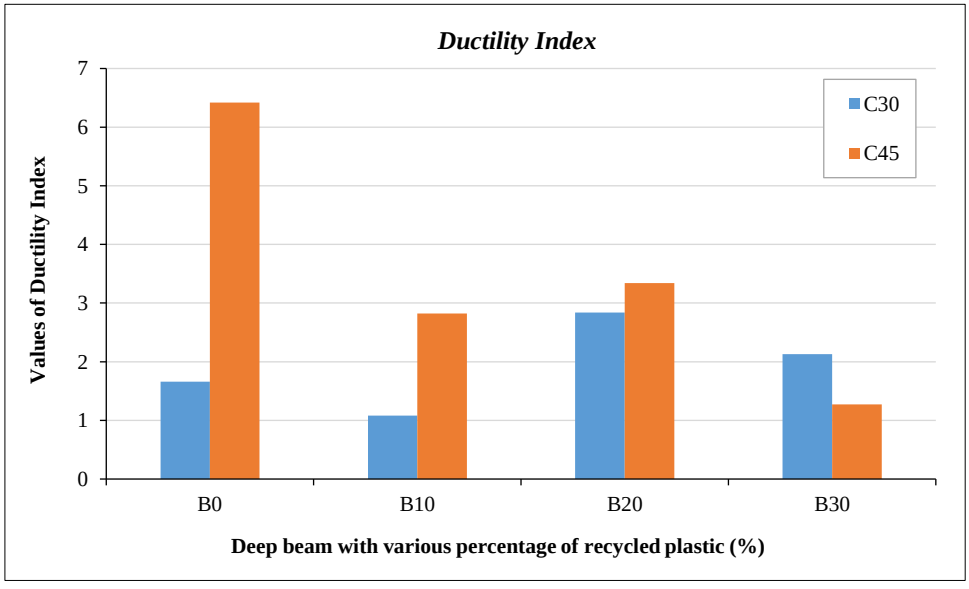

Figure 13. Ductility Index for the Tested Deep Beams

3.5. Stiffness Criteria

Based on the maximum bearing resistance of these beams, the stiffness was calculated by dividing the amount (load/deflection) by 45% of this Resistance, which was then projected onto each curve of the (load-deflection) relationship to find the amount of deflection for each load on the curves [26]. The second slope, drawn on the load-deflection curve in Figure 11 and 12, can be used to determine any part's stiffness requirement, as shown by the R.C.-supported deep beam. According to the results shown in Figure 14, every tested deep beam with a plastic waste

percentage of 10% or 20% had more stiffness than the reference specimen, except for 30%. The evaluation of the plastic garbage resulted in a 14.5 percent drop from the reference. There was likewise a difference in the second group: although the percentage (20%) fell by 15% from the reference, the rate (10% and 30%) grew. For deep beams containing 20% of the first group, the impact of (HDPE) plastic waste on stiffness is particularly pronounced.

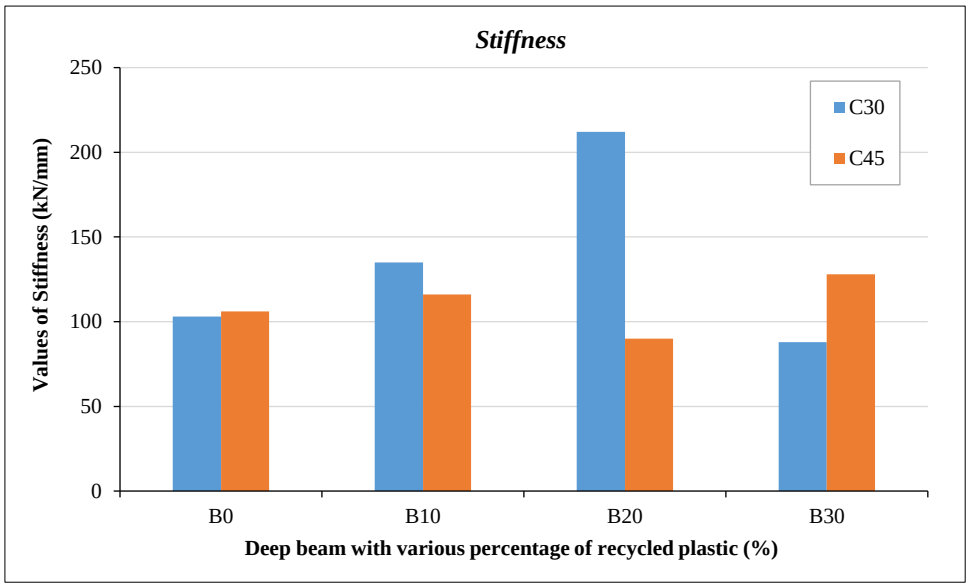

Figure 14. Stiffness Criteria of Deep Beams

4. Theoretical approach

Strut and Tie Model: This method is considered one of the most direct and widely accepted techniques for the analysis and design of deep-reinforced concrete beams, as Figure 15**,** ACI-Code 318-19, delineates this method [27].

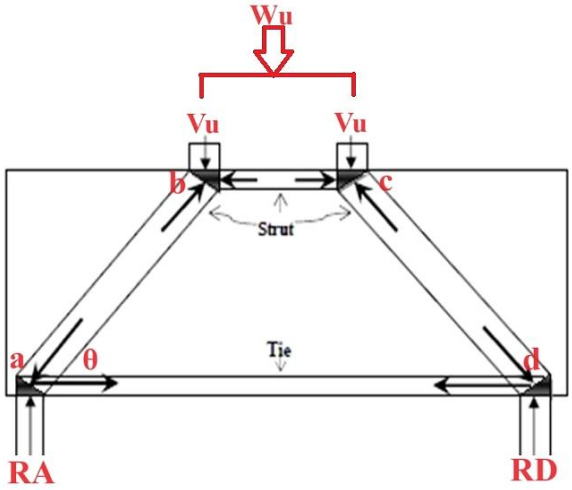

Figure 15. Mechanism of load transmission within the threshold

4.1. Design for Flexural

According to ACI Code 318–19, a deep beam in flexural design is defined as one where the ratio of the clear span lo to the total depth h is less than or equal to 4. Minimum tension reinforcement of the main steel ratio ρ shall not be less than ρ_{min} of Equation 1:

$$\rho_{min} = 1.4/fy \quad (1)$$

where $\rho_{min} = As/bd$; As: is the primary tension reinforcement (mm^2); b: is the beam width (equal to 150 mm); d: is the adequate depth (equal to 0.9 × h = 450 mm); h: is the depth of the beam (equal to 500 mm); and fy is the steel strength (496 N/mm^2); For fy=460 N/mm^2 (about 66500 (lb/in^2)), ρ_{min} is about 0.3%.

ρ_{min}=1.4/496 = 0.00282 → ρ_{min}=As/bd = 0.00282 = As / 150 × 450

As= 191 mm^2 Use 2ø12 As = π/4 × 122 × 2= 226 < 191 O.K.

4.2. Design for Shear

The shear restrictions of ACI Code 318–19 pertain to top-loaded simple or continuous beams with a clear span to effective depth ratio (lo/d) of less than 4, necessitating an orthogonal mesh of web reinforcement. The minimum areas of the vertical and horizontal bars must comply with Equations 2 and 3.

$$Av_{min} = 0.0025 \times b \times s \quad (2)$$

where; Av: is the reinforcement area of the vertical bar; b: is the beam width (equal to 150 = mm); s: is the spacing between bar c/c when $s = d/5$ or 300; Where d is (height - $Tie\ width$ /2).

$$Avh_{min} = 0.0015 \times b \times s \quad (3)$$

where; Avh is the reinforcement area of the horizontal bar; b and S were explained previously:

where d = 500 – 240 / 2 = 380 mm = 380/5 = 78 mm → Use min. between 78 and 300, so use s = 78 mm

$\therefore Av_{min}$ = 0.0025 × 150 ×78 = 30 mm^2

Use ø 8 @225 mm → When S = 100 × 78/30 = 260 < 225 O.K.

Also Avh_{min}=0.0015×150×78 = 18 mm^2

Use ø 8 @150 mm → When S = 100 × 78/18 = 434 < 150 O.K.

4.3. Analysis of Deep Beam

By examining the strut force ($Fnsab$), we determine the response force, and by the equilibrium between the reaction force and the vertical load force, we ascertain the applied force.

$$Wt = (As \times Fy)/fn(ab) \times b \quad (4)$$

where: Wt: width of tie; As: is the primary tension reinforcement (226 mm^2); Fy: is the steel strength (496 N/mm^2); $fn(ab)$: is the strength of strut ab as shown in Figure 14**;** b: is the beam width (equal to 150 mm):

$$fnab = 0.85 \times f\acute{c} \times \beta n(\beta s) \quad (5)$$

where: $f\acute{c}$: Compressive strength of concrete; βs: A coefficient that depends on the shape of the support; βn: A coefficient that depends on the type of forces meeting at a point; $\beta n = 1.0$ When the node (C-C-C); $\beta n = 0.8$ When the node (C-C-T); $\beta n = 0.6$ When the node (C-T-T); $\beta s = 1.0$ for Prismatic Strut.

$fnab$ =0.85 × 45 × 0.8 = 30.6 MPa → Wt = (226×496) / (30.6×150) = 24.44 mm

Z = 0.8 × d

where: d: is the distance from the edge of the compression zone to the center of the tension reinforcement (adequate depth).

d=0.9 × h → h is the depth of the beam (Equal to 500 mm)

d=0.9 × 500 = 450 mm and Z=0.8 × 450 = 360 mm

θ = tan^{-1} (z/shear distance) = tan^{-1} (360/450) → θ= 38.67^o

Wsab b × sinθ + wt × cosθ → Wsab: width of strut

Wsab=150 × sin38.67^o + 24.44 × cos38.67^o = 112.82 mm

Fnab=0.85 × f'c × βn(βs) × b × Wsab

Fnab is the force of strut ab as shown in Figure 15**.**

Fnab=0.85 × 45 × 0.8 × 150 × 112.82 × 10^{-3} = 517.87 KN → ϕ Fnab=0.75 × 517.87 =388.40 KN

RA = RD = Vu= ϕ Fnab × sinθ → Vu: Force in reaction → Vu= 388.40 × sin38.67^o = 242.73 KN

Wu = Vu × 2 → Wu: Applied force → Wu=242.73 × 2 = 485.47 KN

Similarly, for $f\acute{c}$ when it equals 30 MPa

RA = RD = Vu = 175.5 KN → Wu = 175.5 × 2 = 351.01 KN

The prior study revealed that the predicted failure load closely approximates the observed value for deep beams.

5. Conclusions

In the present work, the following inferences may be made in light of the documented test findings from the flexural testing carried out in this investigation:

- Substitutions in the second group were less than 2% lower than the reference beam only for specimen B30. The first group had a 20%, and 30% replacement rate rise in shear failure, while the 10% replacement rate fell by 1.25% compared to the reference specimen. The replacement's favorable environmental effect makes the 23.5% strength drop undesirable, but the 2% ductility reduction is acceptable.
- It is true that there was a discernible improvement; most stiffness replacement rates, except for group C30 specimen B30, were 14% lower than those of the reference, as were group C45B specimen 20, which were 13% lower.
- Except for 10%, deflection rises in the first group as plastic debris proportions increase. This indicates that this plastic has a higher deflection capacity; the most considerable deflection was recorded in the second group at the reference. Because the plasticizer raises the plastic to the surface, the deflection reduces as the replacement rate rises. Consequently, there won't be a deflection ability rate in this case.
- The first group's results are favorable and typically acceptable because of their homogeneity. Because the plastic rose to the surface with the plasticizer, there was no homogeneity in the second group. This impacted the remaining outcomes, producing outcomes that were essentially unanticipated and random.
- The deep beam will acquire more plastic debris because of its large concrete size. This would significantly reduce the amount of non-biodegradable plastic garbage in nature, thereby aiding the environment.

6. Declarations

6.1. Author Contributions

Conceptualization, A.M.A. and O.A.S.; methodology, O.A.S.; software, A.M.A.; validation, A.M.A. and O.A.S.; formal analysis, A.M.A.; investigation, A.M.A. and O.A.S.; resources, O.A.S.; data curation, A.M.A.; writing—original draft preparation, A.M.A.; writing—review and editing, A.M.A. and O.A.S.; visualization, A.M.A. and O.A.S.; supervision, O.A.S.; project administration, O.A.S.; funding acquisition, A.M.A. and O.A.S. All authors have read and agreed to the published version of the manuscript.

6.2. Data Availability Statement

The data presented in this study are available in the article.

6.3. Funding

The authors received no financial support for the research, authorship, and/or publication of this article.

6.4. Acknowledgements

The authors would like to thank the University of Mosul's Civil Engineering Department Head for their support and the Constructional Materials Lab personnel for their help in finishing this study.

6.5. Conflicts of Interest

The authors declare no conflict of interest.

7. References

[1] Franklin Associates. (2011). Cradle-to-gate life cycle inventory of nine plastic resins and four polyurethane precursors. Franklin Associates, A Division of Eastern Research Group, Inc. Prairie Village, United States.

[2] Webb, H. K., Arnott, J., Crawford, R. J., & Ivanova, E. P. (2013). Plastic degradation and its environmental implications with special reference to poly(ethylene terephthalate). Polymers, 5(1), 1–18. doi:10.3390/polym5010001.

[3] Shukur, M. H., Ibrahim, K. A., Al-Darzi, S. Y., & Salih, O. A. (2023). Mechanical properties of concrete using different types of recycled plastic as an aggregate replacement. Cogent Engineering, 10(1). doi:10.1080/23311916.2023.2243735.

[4] Sabariman, B., & Widodo, S. (2024). Effect of Steel Fiber on Plastic Hinge Length of Concrete Columns: Buckingham Theory Application. Civil Engineering Journal (Iran), 10(5), 1386-1408. doi:10.28991/CEJ-2024-010-05-03.

[5] Napper, I. E., & Thompson, R. C. (2020). Plastic Debris in the Marine Environment: History and Future Challenges. Global Challenges, 4(6), 1900081. doi:10.1002/gch2.201900081.

[6] EMF. (2017). Urban Biocycles. The Ellen MacArthur Foundation (EMF), Isle of Wight, United Kingdom. Available online: https://www.ellenmacarthurfoundation.org/cities-urban-biocycles (accessed on 20 October 2025)

[7] Jain, A., Siddique, S., Gupta, T., Jain, S., Sharma, R. K., & Chaudhary, S. (2018). Fresh, Strength, Durability and Microstructural Properties of Shredded Waste Plastic Concrete. Iranian Journal of Science and Technology, Transactions of Civil Engineering, 43(S1), 455–465. doi:10.1007/s40996-018-0178-0.

[8] AL-Darzi, S. Y. K., Ibrahim, K. A., & Salih, O. A. (2024). The Impact Load Behavior of Reinforced Concrete Slab Samples Containing Waste Plastic Aggregate. Tikrit Journal of Engineering Sciences, 31(4), 202–221. doi:10.25130/tjes.31.4.20.

[9] Hassan, B. R., Manguri, A., Hussein, A. B., Corrado, A., Abdulrahman, P. H., Mohammed, L. M., Mahmood, S. S., & Hatim, L. A. (2025). Experimental and numerical assessment of recycled plastic fibers on shear strength and behavior of reinforced concrete beams with basalt FRP bars. Engineering Structures, 330, 119942. doi:10.1016/j.engstruct.2025.119942.

[10] Nilson, H. (1997). Design of Concrete Structures (12th Ed.). McGraw-Hill College, Ohio, United States.

[11] Russo, G., Venir, R., & Pauletta, M. (2005). Reinforced concrete deep beams-shear strength model and design formula. ACI Structural Journal, 102(3), 429. doi:10.14359/14414.

[12] de Paiva, H. A. R., & Siess, C. P. (1965). Strength and Behavior of Deep Beams in Shear. Journal of the Structural Division, 91(5), 19–41. doi:10.1061/jsdeag.0001329.

[13] Smith, K. N., & Vantsiotis, A. S. (1982). Shear Strength of Deep Beams. (1982). ACI Journal Proceedings, 79(3). doi:10.14359/10899.

[14] ECP 203-2018. (2018). Basics of Design and regulations of Construction of Reinforced Concrete Structures: Appendix III, Guide for Testing of Concrete Materials. Egyptian Ministry of Housing, Cairo, Egypt.

[15] ACI CODE-318-19(22). (2019). Building Code Requirements for Structural Concrete and Commentary. American Concrete Institute (ACI), Farmington Hills, United States.

[16] Rahim, N. L., Salehuddin, S., Ibrahim, N. M., Amat, R. C., & Ab Jalil, M. F. (2013). Use of plastic waste (high density polyethylene) in concrete mixture as aggregate replacement. Advanced Materials Research, 701, 265–269. doi:10.4028/www.scientific.net/AMR.701.265.

[17] Shanmugapriya, M., & Santhi, H. (2017). Strength and chloride permeable properties of concrete with high density polyethylene wastes. International Journal of Chemical Sciences, 15(1), 10-17.

[18] Punitha, V., Sakthieswaran, N., & Ganesh Babu, O. (2021). Experimental investigation of concrete incorporating HDPE plastic waste and metakaolin. Materials Today: Proceedings, 37, 1032–1035. doi:10.1016/j.matpr.2020.06.288.

[19] Tamrin, & Nurdiana, J. (2021). The effect of recycled HDPE plastic additions on concrete performance. Recycling, 6(1), 1–19. doi:10.3390/recycling6010018.

[20] Radhi, M. M., Khalil, W. I., & Shafeeq, S. (2022). Flexural behavior of sustainable reinforced concrete beams containing HDPE plastic waste as coarse aggregate. Cogent Engineering, 9(1), 2127470. doi:10.1080/23311916.2022.2127470.

[21] IQS-No. 5. (2019). Portland Cement. Iraqi Standard Specifications (IQS), Baghdad, Iraq.

[22] Shireen, H. H. (2021). Rehabilitation of Lightweight RC Beams with Shear Deficiencies by CFRP. Ph.D. Thesis, University of Kerbala, Karbala, Iraq.

[23] Grimaldi, A., Rinaldi, Z. (2004). Influence of the Steel Properties on the Ductility of R.C. Structures. Novel Approaches in Civil Engineering. Lecture Notes in Applied and Computational Mechanics, vol 14. Springer, Berlin, Germany. doi:10.1007/978-3-540-45287-4_25.

[24] Xie, Y., Ahmad, S. H., Yu, T., Hino, S., & Chung, W. (1994). Shear ductility of reinforced concrete beams of normal and high-strength concrete. Structural Journal, 91(2), 140-149. doi:10.14359/4592.

[25] Sharma, G., Zhao, Z., Sarker, P., Nail, B. A., Wang, J., Huda, M. N., & Osterloh, F. E. (2016). Electronic structure, photovoltage, and photocatalytic hydrogen evolution with p-CuBi2O4 nanocrystals. Journal of Materials Chemistry A, 4(8), 2936–2942. doi:10.1039/c5ta07040f.

[26] Abed, H. S., & Al-Sulayfani, B. J. (2023). Experimental and analytical investigation on effect of openings in behavior of reinforced concrete deep beam and enhanced by CFRP laminates. Structures, 48, 706–716. doi:10.1016/j.istruc.2023.01.013.

[27] ACI CODE-318-19(22). (2019). Building Code Requirements for Structural Concrete and Commentary. American Concrete Institute (ACI), Farmington Hills, United States.